ISSN 1063-7710, Acoustical Physics, 2016, Vol. 62, No. 3, pp. 292–299. © Pleiades Publishing, Ltd., 2016.

CLASSICAL PROBLEMS OF LINEAR ACOUSTICS AND WAVE THEORY

Wave Propagation Characteristics of Helically Orthotropic Cylindrical Shells and Resonance Emergence in Scattered Acoustic Field. Part 1. Formulations[1]

Majid Rajabi

Department of Mechanical Engineering, Iran University of Science and Technology, Narmak, Tehran, Iran
e-mail: majid_rajabi@iust.ac.ir

Received June 19, 2014

Abstract—The method of wave function expansion is adopted to study the three dimensional scattering of a plane progressive harmonic acoustic wave incident upon an arbitrarily thick-walled helically filament-wound composite cylindrical shell submerged in and filled with compressible ideal fluids. An approximate laminate model in the context of the so-called state-space formulation is employed for the construction of T-matrix solution to solve for the unknown modal scattering coefficients. Considering the nonaxisymmetric wave propagation phenomenon in anisotropic cylindrical components and following the resonance scattering theory which determines the resonance and background scattering fields, the stimulated resonance frequencies of the shell are isolated and classified due to their fundamental mode of excitation, overtone and style of propagation along the cylindrical axis (i.e., clockwise or anticlockwise propagation around the shell) and are identified as the helically circumnavigating waves.

Keywords: wave propagation; state-space formulations; surface waves

DOI: 10.1134/S1063771016030143

1. INTRODUCTION

It is not more than two decade that *Resonance Acoustic Spectroscopy* (RAS) technique has been proven to be an effective tool for material characterization purposes and non-destructive testing/evaluation of materials [1–6], remote classification of submerged targets [3, 4, 7], and on-line monitoring of elastic components [8, 9]. In this technique, the dependency of the resonance features of the target component to its bulk physical properties such as stiffness matrix, density and geometrical parameters are utilized to set an inverse scattering solution, in order to evaluate the objective property of the component by correlating the measured spectra to the theoretical ones through iterative numerical algorithms. Therefore, this technique is necessitous to the complicated resonance response function expected from an even undamaged target component. Hence, a theoretical resonance scattering model and a good understanding of the resonance excitation phenomenon is essential [10–15].

Cylindrical components are frequently used in practical engineering. Consequently, there have been several research works on their acoustic response, and in particular, the scattering of acoustic waves from such structures has been an active area of research for over a century. The first pioneering investigation of acoustic wave scattering from submerged solid elastic cylinders based on a normal-mode expansion dates back to Faran [15]. The three dimensional analysis of the problem when the propagation direction of the incident wave makes an arbitrary angle with the normal to the cylinder, was considered by Flax et al. [16]. The similar problem for a cylindrical shell was studied by Veksler [14]. Comprehensive reviews of these topics and extensive bibliographies can be found in the works of Gaunaurd [12], Uberall [13], and Veksler [14].

The increased use of anisotropic materials in practical engineering has led to activities in this area in recent decade. Honarvar and Sinclair [17] developed an exact normal-mode expansion for the scattering of a compression acoustic wave from an immersed, transversely isotropic solid cylinder. Kaduchak and Loeffler [18] used the exact 3D elasticity theory to examine acoustic scattering from a multilayered transversely isotropic cylindrical shell excited by an obliquely incident plane wave. Ahmad and Rahman [19] developed normal mode expansions to investigate the effect of the angle of incidence on the scattering of an acoustic wave by a transversely isotropic cylinder immersed in a fluid. They exposed three critical angles (in spite of two common critical angles of isotropic cases) of incidence of a transversely isotropic cylindrical cylinder. Kim and Ih [3] extended Honarvar and Sinclair's [17] work by using the normal mode expan-

[1] The article is published in the original.

sion technique to present a resonance scattering analysis for oblique incidence of a plane acoustic wave upon an air-filled, transversely isotropic cylindrical shell immersed in water, with application to material characterization. Hasheminejad and Rajabi [4] used the laminate approximate model in the context of state space formulation to study the acoustic scattering problem from a submerged orthotropic cylindrical shell. They extend their work to the laminated case along with the RST-approach to investigate the imperfect bonding effects on excited resonance frequencies [6]. Kleshchev [20, 21] derived the characteristic equations for determination of phase velocities of the elastic wave propagation phenomenon in the transversely isotropic and orthotropic thin walled cylindrical shells. Karabutov et al. [22] employed a wideband acoustic spectroscopy with a laser ultrasound source for quantitative analysis of the effect of porosity on the attenuation coefficient of longitudinal acoustic waves in carbon fiber reinforced plastic (CFRP) composite materials. Polikarpova et al. [23] discussed the dependence of the polarization of acoustic waves on the propagation direction with respect to the crystal axes of a tellurium crystal.

In particular, fiber reinforced composite cylinders and cylindrical shells have been used as novel types of structures providing elevated performance because of their adaptability in providing enhanced mechanical properties and lightweight. Because such materials demonstrate often highly anisotropic behaviour (helical orthotropy or monoclinic anisotropy), it is difficult to evaluate the material mechanical properties or to monitor the state of health or failure, especially in the state of operation, by usual methods. The authors believe to the applicability of RAS-technique for resonance isolation and classification of highly anisotropic cylindrical shells. The purpose of the present study is to theoretically ensure about their belief by presenting a theoretical solution for the scattering problem based on the exact three-dimensional anisotropic elasticity and proposing a novel resonance classification and identification scheme founded on the wave propagation characteristics of the body. For this idea, a laminate approximate model along with the so-called state-space formulation in conjunction with the transfer matrix approach are used to investigate the resonance scattering phenomenon of a filament-wound cylindrical shell of arbitrary thickness. This paper is dedicated to the formulation of the work as the part 1. In the second part, the numerical results are discussed.

2. FORMULATION

Consider a time harmonic infinite plane acoustic wave, with the circular frequency ω, obliquely incident at an angle α on a submerged and fluid-filled helically filament-wound cylindrical shell of infinite length, inner radius a_0 and outer radius a_q. The problem geometry is depicted in Fig. 1, where (x, y, z) is the

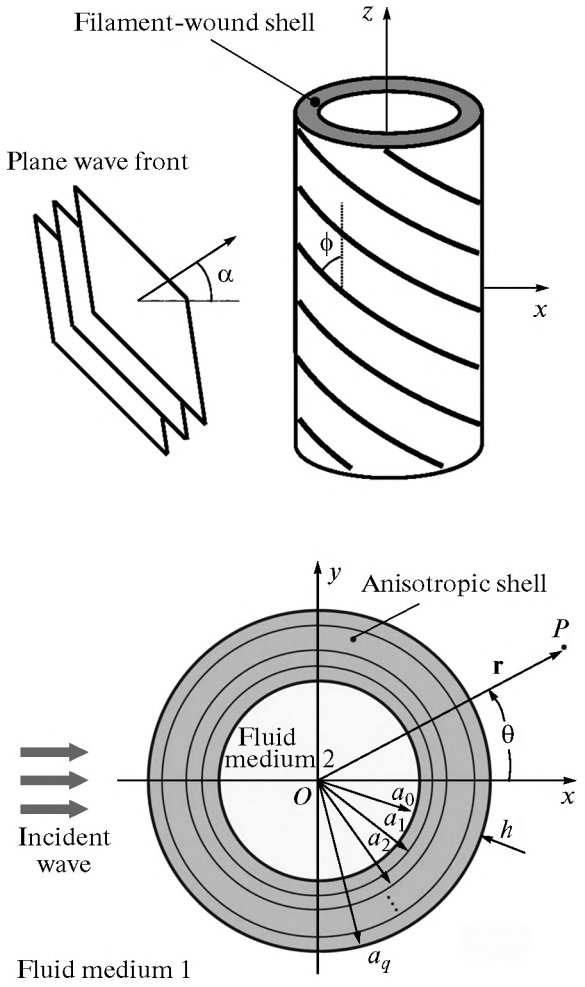

Fig. 1. Configuration of problem.

Cartesian coordinate system with origin at O, the z direction is coincident with the axis of the cylindrical shell, and (r, θ) is the corresponding cylindrical polar coordinate system.

2.1. Acoustic Field Equations

Following the standard methods of theoretical acoustics, the field equations for an inviscid and ideal compressible medium that cannot support shear stresses may conveniently be expressed in terms of a scalar velocity potential as [24]

$$\mathbf{v} = -\nabla\varphi, p = \rho\frac{\partial\varphi}{\partial t}, \nabla^2\varphi + k^2\varphi = 0, \quad (1)$$

where $\mathbf{v}$ is the fluid particle velocity vector, p is the acoustic pressure, ρ is the ambient density, $k = \omega/c$ is the wave number for the dilatational wave, c is the speed of sound.

The expansion of the plane progressive incident wave field, propagating in the surrounding fluid

medium, in cylindrical coordinate (see Fig. 1) has the form [24]

$$\varphi_{\text{inc}}(r,\theta,\omega) = \varphi_0 \sum_{n=0}^{\infty} \varepsilon_n i^n J_n(k_r r)\cos(n\theta) e^{i(k_z z-\omega t)}, \quad (2)$$

where $k_z = k\sin\alpha$, $k_r = k\cos\alpha$, $k = \omega/c_1$ is the wave number in the outer fluid medium 1 (see Fig. 1), φ_0 is the amplitude of the incident wave, symbol n is the Neumann factor ($\varepsilon_n = 1$ for $n = 0$, and $\varepsilon_n = 2$ for $n > 0$), $i = \sqrt{-1}$, $J_n(x)$ is the cylindrical Bessel function of the first kind of order n. The solutions of the Helmholtz equation for the scattered potential in the surrounding fluid medium 1, and the transmitted potential in the inner fluid medium 2 can respectively be expressed as a linear combination of cylindrical waves as [24]

$$\begin{aligned}
&\varphi_1(r,\theta,\omega)\\
&= \sum_{n=0}^{\infty} \varepsilon_n i^n \left[A_n(\omega)\cos(n\theta) + B_n(\omega)\sin(n\theta)\right]\\
&\qquad \times H_n^{(1)}(k_r r) e^{i(k_z z-\omega t)},\\
&\varphi_2(r,\theta,\omega)\\
&= \sum_{n=0}^{\infty} \varepsilon_n i^n \left[C_n(\omega)\cos(n\theta) + D_n(\omega)\sin(n\theta)\right]\\
&\qquad \times J_n(K_r r) e^{i(k_z z-\omega t)},
\end{aligned} \quad (3)$$

where $K_r = \sqrt{K^2 - k_z^2}$, $K = \omega/c_2$ is the acoustic wave number in the inner medium 2, $H_n^{(1)}(x) = J_n(x) + iY_n(x)$ is the cylindrical Hankel function of the first kind of order n, $Y_n(x)$ is the cylindrical Bessel function of the second kind of order n, (A_n, B_n) and (C_n, D_n) are unknown scattering/transmission coefficients.

2.2. State-space Formulation

In a linearly elastic continuum, the equations of motion, in the absence of body forces, in terms of the stress components σ_{ij} may be written as [25–27]

$$\frac{\partial \mathbf{Y}}{\partial r} = \mathbf{M}\mathbf{Y}, \quad (4)$$

where $\mathbf{Y} = [u_z, u_\theta, u_r, \sigma_{rr}, \sigma_{r\theta}, \sigma_{rz}]^T$ is the state vector, u_r, u_θ and u_z are the material displacements in the r, θ and z directions respectively and M is a 6×6 coefficient matrix whose elements are provided in Appendix I. The state vector Y can be expanded in terms of unknown modal coefficients, by employing the appropriate normal mode expansions, as

$$\begin{aligned}
\mathbf{Y} &= \begin{Bmatrix} u_z \\ u_\theta \\ u_r \\ \sigma_{rr} \\ \sigma_{r\theta} \\ \sigma_{rz} \end{Bmatrix}\\
&= \sum_{n=0}^{\infty} \begin{Bmatrix} a_q\left[\nu_{z,n}(\eta)\cos(n\theta) + w_{z,n}(\eta)\sin(n\theta)\right] \\ a_q\left[\nu_{\theta,n}(\eta)\cos(n\theta) + w_{\theta,n}(\eta)\sin(n\theta)\right] \\ a_q\left[\nu_{r,n}(\eta)\cos(n\theta) + w_{r,n}(\eta)\sin(n\theta)\right] \\ c_{44}\left[\Sigma_{rr,n}(\eta)\cos(n\theta) + \Gamma_{rr,n}(\eta)\sin(n\theta)\right] \\ c_{44}\left[\Sigma_{r\theta,n}(\eta)\cos(n\theta) + \Gamma_{r\theta,n}(\eta)\sin(n\theta)\right] \\ c_{44}\left[\Sigma_{rz,n}(\eta)\cos(n\theta) + \Gamma_{rz,n}(\eta)\sin(n\theta)\right] \end{Bmatrix} e^{i(k_z z-\omega t)},
\end{aligned} \quad (5)$$

where $\eta = r/a_q$ is the dimensionless radial coordinate. Subsequently substituting (5) into (4) and utilizing the orthogonality of trigonometric functions, we obtain

$$\frac{d\mathbf{V}_n}{d\eta} = \mathbf{G}_n(\eta)\mathbf{V}_n, \quad (6)$$

where $\mathbf{V}_n = \left[\nu_{z,n}, w_{\theta,n}, \nu_{r,n}, \Sigma_{rr,n}, \Gamma_{r\theta,n}, \Sigma_{rz,n}, w_{z,n}, \nu_{\theta,n}, w_{r,n}, \Gamma_{rr,n}, \Sigma_{r\theta,n}, \Gamma_{rz,n}\right]^T$ is the modal state variables vector and $\mathbf{G}_n$ is a 12×12 modal coefficient matrix whose elements are functions of the radial coordinate η and can be easily derived.

2.3. Transfer Matrix Solution

At this point, we shall consider the solution to the state Eq. (6) by adopting a laminate approximate model: the cylindrical shell is discretized into q sublayers of equal thickness, $h_q = h/q$ (i.e., $h = a_q - a_0$ is the total thickness of the shell) with the outer radius of the m-th sublayer being $a_m = a_0 + mh_q$ where $m = 0, \ldots, q$. All sublayers are perfectly bonded at their interfaces and lined up such that their axes of symmetry coincide with each other (see Fig. 1). As the thickness of each layer is supposed to be very small, the coefficient matrix $\mathbf{G}_n$ can be assumed constant within each layer, which we denote as $\mathbf{G}_n(\eta_{m-1})$ for the m-th layer. Thus, within the m-th layer, the solution to Eq. (6) can be written as

$$\begin{aligned}
&\mathbf{V}_n(\eta)\\
&= \mathbf{V}_n(\eta_{m-1})\exp\left[(\eta - \eta_{m-1})\mathbf{G}_n(\eta_{m-1})\right],
\end{aligned} \quad (7)$$

where $\left(\eta_{m-1} = \left[a_0 + (m-1)\eta_q\right]/a_q\right) \le \eta \le \left(\eta_m = \left[a_0 + mh_q\right]/a_q\right)$, and $m = 1, \ldots, q$. Subsequent evaluation of

Eq. (7) at the outer surface of the m-th layer, leads to the following useful recurrence relation:

$$\mathbf{V}_n(\eta_m) = \mathbf{V}_n(\eta_{m-1})\exp\left[h_q\,\mathbf{G}_n(\eta_{m-1})/a_q\right], \tag{8}$$

which relates the state variables at the outer surface of the m-th layer to those at the inner surface. At last, by invoking the continuity conditions between all assuming layers, the state variables at the outer radius of the cylindrical shell (i.e., at $r = a_q$ for which $\eta_q = a_q/a_q = 1$) are favourably related to those at the inner radius (i.e., at $r = a_0$ for which $\eta_0 = a_0/a_q$) via a 12×12 global modal transfer matrix n, by

$$\mathbf{V}_n(\eta_q) = \mathbf{T}_n\mathbf{V}_n(\eta_0), \tag{9}$$

where $T_n = \prod_{m=1}^{q}\exp\left[h_q\,G_n(\eta_{m-1})/a_q\right]$.

2.4. Boundary Conditions

The unknown coefficients (A_n, B_n) and (C_n, D_n), as well as the unknown elements of the modal state variable vectors at the inner surface of the cylindrical shell, $\mathbf{V}_n(\eta_0) = \left[\nu^0_{z,n}, w^0_{\theta,n}, \nu^0_{r,n}, \Sigma^0_{rr,n}, w^0_{z,n}, \nu^0_{\theta,n}, w^0_{r,n}, \Gamma^0_{rr,n}\right]^T$, must be determined from the appropriate boundary conditions imposed at the inner and the outer surfaces of the shell. Thus, assuming continuity of normal fluid and solid velocities, normal stress and fluid pressure, and vanishing of tangential stress at $r = a_0$ and $r = a_q$ imply that

$$\begin{aligned}
&(-i\omega)\,u_r(r,\theta,\omega)\big|_{r=a_0,a_q} = \nu_r(r,\theta,\omega)\big|_{r=a_0,a_q},\\
&\sigma_{rr}(r,\theta,\omega)\big|_{r=a_0,a_q} = -p(r,\theta,\omega)\,|_{r=a_0,a_q},\\
&\sigma_{r\theta}(r,\theta,\omega)\big|_{r=a_0,a_q} = \sigma_{rz}(r,\theta,\omega)\big|_{r=a_0,a_q} = 0.
\end{aligned} \tag{10}$$

Ultimately, by making use of (1)–(3) and (9) in (10), we obtain

$$\mathbf{Z}_n\mathbf{X}_n = \mathbf{W}_n, \tag{11}$$

where $\mathbf{X}_n = [A_n, C_n, \nu^0_{z,n}, w^0_{\theta,n}, \nu^0_{r,n}, \Sigma^0_{rr,n}, B_n, D_n, w^0_{z,n}, \nu^0_{\theta,n}, w^0_{r,n}, \Gamma^0_{rr,n}]^T$ is the unknown modal vector, $\mathbf{Z}_n$ is a 12×12 matrix and $\mathbf{W}_n$ is a 12×1 vector, which elements are given in Appendix II.

2.5. The Global and Resonance Scattering Coefficients

The most applicable field quantities associated with acoustic resonance scattering are the total (global) and resonance scattering coefficients. The total scattering coefficient may be obtained from the standard definition of the backscattering form-function amplitude, which is written as [14]

$$\begin{aligned}
\left|f_\infty(\theta=\pi,\omega)\right| &\approx \lim_{r\to\infty}\sqrt{\frac{2r}{a_q}}\left|\frac{\varphi_1(r,\theta=\pi,\omega)}{\varphi_{\text{inc}}}\right|\\
&= \left|\sum_{n=0}^{\infty} f_n(\theta=\pi,ka_q)\right|,
\end{aligned} \tag{12}$$

where

$$f_n(\theta,ka_q) = \frac{2\varepsilon_n}{\sqrt{\pi ika_q}}\left[A_n\cos(n\theta) + B_n\sin(n\theta)\right] \tag{13}$$

is referred to as the total scattering coefficient corresponding to n-th partial wave. The pure resonance contribution in the scattering amplitudes of the n-th mode can be isolated by subtracting the background (geometrical) effect from the total form function as follows [14]:

$$\left|f_n^{(\text{res})}(\theta,ka_q)\right| = \left|f_n(\theta,ka_q) - f_n^{(b)}(\theta,ka_q)\right|, \tag{14}$$

where the inherent background coefficients are defined as

$$f_n^{(b)}(\theta,ka_q) = \frac{2\varepsilon_n}{\sqrt{\pi ika_q}}A_n^{(b)}\cos(n\theta), \tag{15}$$

in which $A_n^{(b)}$ is the proper background scattering coefficient. In order to obtain the background scattering coefficients, $A_n^{(b)}$, the "*inherent background approach*" [28] is employed. The inherent background scattering coefficients are given as [28, 29]

$$A_n^{(b)} = -\frac{k_r a_q J_n'(k_r a_q) - J_n(k_r a_q)\Omega_n}{k_r a_q H_n^{(1)\prime}(k_r a_q) - H_n^{(1)}(k_r a_q)\Omega_n}, \tag{16}$$

where

$$\Omega_n = \begin{cases} \dfrac{\rho_1}{\rho_c}\dfrac{n^2 + Q(n\rho_c/\rho_2)}{Q + (n\rho_c/\rho_2)}, & n \neq 0,\\[2ex] \dfrac{4\rho_1}{\rho_2 - 4\rho_c\ln(b/a)}, & n = 0, \end{cases} \tag{17}$$

in which $Q = n\dfrac{1+(b/a)^{2n}}{1-(b/a)^{2n}}$.

2.6. Wave Propagation Characteristics

The wave propagation along the anisotropic cylindrical shell can be classified into the helically clockwise and anticlockwise waves propagating around the shell (See Fig. 2) at the circular frequency of ω, with the axial wavelength of $2\pi/k_z$ and helix angle of $\Psi = \tan^{-1}(k_z a/n)$. The state variables may be represented as

$$\mathbf{Y}^{\pm} = \begin{Bmatrix} u_z\\ u_\theta\\ u_r\\ \sigma_{rr}\\ \sigma_{r\theta}\\ \sigma_{rz} \end{Bmatrix} = \sum_{n=0}^{\infty}\begin{Bmatrix} a_q\overline{u}_{z,n}(\eta)\\ a_q\overline{u}_{\theta,n}(\eta)\\ a_q\overline{u}_{r,n}(\eta)\\ c_{44}\overline{\sigma}_{rr,n}(\eta)\\ c_{44}\overline{\sigma}_{r\theta,n}(\eta)\\ c_{44}\overline{\sigma}_{rz,n}(\eta) \end{Bmatrix} e^{-i(k_z z \pm n\theta - \omega t)}, \tag{18}$$

where "+" refers to the anti-clockwise wave propagation and "–" refers to the clockwise wave propagation type. Introducing these state variables into Eq. (4) and following the same procedure that is done for the scat-

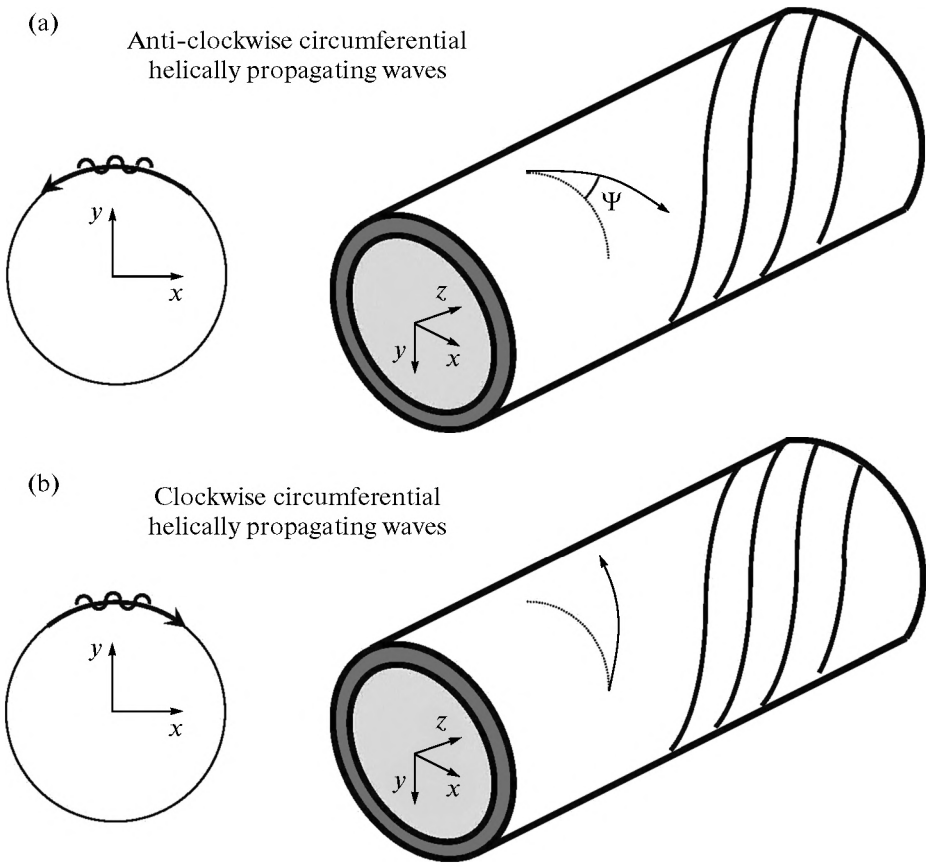

Fig. 2. Clockwise and anti-clockwise circumferential helically propagating wave modes.

tering problem, the state variables at the outer and inner surfaces of m-th sublayer are related by $\overline{\mathbf{V}}_n^{\pm}(\eta_m) = \exp\left[h_q\, \mathbf{G}_n^{\pm}(\eta_{m-1})/a_q\right]\overline{\mathbf{V}}_n^{\pm}(\eta_{m-1})$, where the elements of $\mathbf{G}_n^{\pm}(\eta)$ are given in Appendix III and $\overline{\mathbf{V}}_n = [\overline{u}_{z,n}, \overline{u}_{\theta,n}, \overline{u}_{r,n}, \overline{\sigma}_{rr,n}, \overline{\sigma}_{r\theta,n}, \overline{\sigma}_{rz,n}]^T$ is the modal state variable vector. The global wave propagation transfer matrix is also calculated as $\overline{\mathbf{T}}_n^{\pm} = \prod_{m=1}^{q} \exp\left[h_q\, \mathbf{G}_n^{\pm}(\eta_{m-1})/a_q\right]$ which connects the modal state variable vector at the inner and outer surfaces of the shell, $\overline{\mathbf{V}}_n^{\pm}(\eta_q) = \overline{\mathbf{T}}_n^{\pm}\, \overline{\mathbf{V}}_n^{\pm}(\eta_0)$. The scattered and transmitted velocity potential functions are also defined as

$$\varphi_1^{\pm}(r,\theta,\omega) = \sum_{n=0}^{\infty} \varepsilon_n i^n A_n(\omega)\, H_n^{(1)}(k_r r)\, e^{i(k_z z \pm n\theta - \omega t)},$$
$$\varphi_2^{\pm}(r,\theta,\omega) = \sum_{n=0}^{\infty} \varepsilon_n i^n B_n(\omega)\, J_n(K_r r)\, e^{i(k_z z \pm n\theta - \omega t)}. \tag{19}$$

Implementing the transformation relations in the boundary conditions, Eq. (10), and neglecting the incident wave field, $\varphi_{\text{inc}} = 0$, it can be easily shown that the wave propagation characteristic equation is obtained as

$$\mathbf{\Lambda}_n^{\pm}\, \overline{\mathbf{X}}_n = 0, \tag{20}$$

where $\mathbf{\Lambda}_n^{\pm}$ is a 6×6 matrix as

$$\Lambda_n^{\pm} = \begin{bmatrix} 0 & \Lambda_{n,12}^{\pm} & -T_n^{\pm(1.1)} & -T_n^{\pm(1.2)} & 1 & 0 \\ 0 & \Lambda_{n,22}^{\pm} & -T_n^{\pm(2.1)} & -T_n^{\pm(2.2)} & 0 & 1 \\ \Lambda_{n,31}^{\pm} & \Lambda_{n,32}^{\pm} & -T_n^{\pm(3.1)} & -T_n^{\pm(3.2)} & 0 & 0 \\ \Lambda_{n,41}^{\pm} & \Lambda_{n,42}^{\pm} & -T_n^{\pm(4.1)} & -T_n^{\pm(4.2)} & 0 & 0 \\ 0 & \Lambda_{n,52}^{\pm} & -T_n^{\pm(5.1)} & -T_n^{\pm(5.2)} & 0 & 0 \\ 0 & \mathrm{L}_{n,62}^{\pm} & -T_n^{\pm(6.1)} & -T_n^{\pm(6.2)} & 0 & 0 \end{bmatrix}, \tag{21}$$

$$\mathbf{\Lambda}_{n,j2}^{\pm} = -T_n^{\pm(j,3)}\left(K_r \varepsilon_n i^{n-1} J_n'(K_r a_0)/\omega a_q\right) - T_n^{\pm(j,4)}\left(\omega \rho_2 \varepsilon_n i^{n+1} J_n(K_r a_0)/c_{44}\right), \quad j = 1,\ldots,6, \tag{22}$$

$$\mathbf{\Lambda}_{n,31}^{\pm} = K_r \varepsilon_n i^{n-1} J_n'(K_r a_0)/\omega a_q,$$
$$\mathbf{\Lambda}_{n,41}^{\pm} = \omega \rho_2 \varepsilon_n i^{n+1} J_n(K_r a_0)/c_{44},$$

and $\bar{\mathbf{X}}_n = \left[A_n, B_n, \bar{u}^0_{z,n}, \bar{u}^0_{\theta,n}, \bar{u}^1_{z,n}, \bar{u}^1_{\theta,n}\right]^T$ is the unknown modal vector. Remember that the superscripts 0 and 1 imply the modal normalized state variables at the inner and outer radii of the shell. The nontrivial solution of the above relation is found by setting the determinant of the coefficient matrix equal to zero; i.e., $\left|\mathbf{\Lambda}^{\pm}_n\right| = 0$, and searching for its frequency-wavelength ($ka_q = \omega a_q/c_1, k_z a_q$) roots.

This completes the background required for the acoustic scattering analysis of a submerged and fluid-filled filament-wound cylindrical shell via the resonance scattering theorem.

4. CONCLUSIONS

The novel features of a state-space method in conjunction with the transfer matrix approach are used to present an exact analysis based on the wave function expansion to study the scattering of a plane harmonic acoustic wave incident at an arbitrary angle upon a helically filament-wound (fiber-reinforced composite) cylindrical shell, submerged in and filled with compressible ideal fluids. Using the classic acoustic resonance scattering theory along with the extracted dispersion curves associated to the anticipated wave propagation phenomenon in the anisotropic cylindrical body, a novel methodology has been proposed to classify the isolated resonance modes according their wave propagation direction (clockwise or anti-clockwise with respect to the cross section of the cylindrical body) and subsequently to identify them as the resonance modes of the body.

Finally, the author is hopeful that the proposed approach may be considered as an essential tool in the complex process of material characterization, nondestructive testing and evaluation, remote classification, and on-line monitoring of mechanical properties of composite cylindrical components which are of practical importance in numerous industrious applications.

APPENDIX I

$$\mathbf{M} = \begin{bmatrix} \mathbf{M}_{11} & \mathbf{M}_{12} & \mathbf{M}_{13} \\ \mathbf{M}_{21} & \mathbf{M}_{22} & \mathbf{M}_{23} \\ \mathbf{M}_{31} & \mathbf{M}_{32} & \mathbf{M}_{33} \end{bmatrix},$$

where

$$\mathbf{M}_{11} = \begin{bmatrix} 0 & 0 \\ 0 & \frac{1}{\eta} \end{bmatrix}, \mathbf{M}_{12} = \begin{bmatrix} -a_q\gamma & 0 \\ -\frac{\beta}{\eta} & 0 \end{bmatrix}, \mathbf{M}_{13} = \begin{bmatrix} -\frac{c_{56}}{\kappa_1} & \frac{c_{66}}{\kappa_1} \\ \frac{c_{55}}{\kappa_1} & -\frac{c_{56}}{\kappa_1} \end{bmatrix}, \mathbf{M}_{23} = \begin{bmatrix} 0 & 0 \\ -\frac{\beta}{\eta} & -\gamma a_q \end{bmatrix},$$

$$\mathbf{M}_{21} = \begin{bmatrix} -\frac{c_{13}a_q\gamma}{c_{11}} - \frac{c_{14}\beta}{c_{11}\eta} & -\frac{c_{14}a_q\gamma}{c_{11}} - \frac{c_{12}\beta}{c_{11}\eta} \\ \frac{\kappa_2\beta}{\eta^2} + \frac{\kappa_3 a_q\gamma}{\eta} & \frac{\kappa_4\beta}{\eta^2} + \frac{\kappa_2 a_q\gamma}{\eta} \end{bmatrix}, \mathbf{M}_{22} = \begin{bmatrix} -\frac{c_{12}}{c_{11}\eta} & \frac{c_{44}}{c_{11}} \\ \frac{\kappa_4}{\eta^2} + \frac{\rho_c a_q^2\tau^2}{c_{44}} & \frac{1}{\eta}\left(\frac{c_{12}}{c_{11}} - 1\right) \end{bmatrix},$$

$$\mathbf{M}_{31} = \begin{bmatrix} -\kappa_5 a_q^2\gamma^2 - \frac{a_q\gamma\beta}{c_{44}\eta}(\kappa_3 + \kappa_6) - \frac{\kappa_2\beta^2}{\eta^2} & \frac{\rho_c a_q^2\tau^2}{c_{44}} - \frac{2a_q\gamma\beta\kappa_2}{\eta} - \kappa_6 a_q^2\gamma^2 - \frac{\kappa_4\beta^2}{\eta^2} \\ \frac{\rho_c a_q^2\tau^2}{c_{44}} - \frac{\kappa_6\beta^2}{\eta^2} - \kappa_7 a_q^2\gamma^2 - \frac{2\kappa_5 a_q\gamma\beta}{\eta} & -\frac{\kappa_2\beta^2}{\eta^2} - \frac{a_q\gamma\beta}{\eta}(\kappa_3 + \kappa_6) - \kappa_5 a_q^2\gamma^2 \end{bmatrix},$$

$$\mathbf{M}_{32} = \begin{bmatrix} -\frac{\kappa_2 a_q\gamma}{\eta} - \frac{\kappa_4\beta}{\eta^2} & -\frac{c_{12}\beta}{c_{11}\eta} - \frac{c_{14}a_q\gamma}{c_{11}} \\ -\frac{\kappa_2\beta}{\eta^2} - \frac{\kappa_3 a_q\gamma}{\eta} & -\frac{c_{14}\beta}{c_{11}\eta} - \frac{c_{13}a_q\gamma}{c_{11}} \end{bmatrix}, \mathbf{M}_{33} = \begin{bmatrix} -\frac{2}{\eta} & 0 \\ 0 & -\frac{1}{\eta} \end{bmatrix},$$

in which $\beta = \frac{\partial}{\partial\theta}$, $\gamma = \frac{\partial}{\partial z}$, $\tau = \frac{\partial}{\partial t}$, and

$$\kappa_1 = \frac{c_{55}c_{66}}{c_{44}} - \frac{c_{56}^2}{c_{44}}, \kappa_2 = \frac{c_{24}}{c_{44}} - \frac{c_{12}c_{14}}{c_{11}c_{44}}, \kappa_3 = \frac{c_{23}}{c_{44}} - \frac{c_{12}c_{13}}{c_{11}c_{44}},$$

$$\kappa_4 = \frac{c_{22}}{c_{44}} - \frac{c_{12}^2}{c_{11}c_{44}},$$

$$\kappa_5 = \frac{c_{34}}{c_{44}} - \frac{c_{13}c_{14}}{c_{11}c_{44}}, \kappa_6 = \frac{c_{44}}{c_{44}} - \frac{c_{14}^2}{c_{11}c_{44}}, \kappa_7 = \frac{c_{33}}{c_{44}} - \frac{c_{13}^2}{c_{44}c_{11}},$$

where c_{ij} are functions of material elastic constants and the angle of filaments from the axis of cylindrical shell, ϕ, given in [30, 31].

APPENDIX II

$$\mathbf{Z}_n = \begin{bmatrix}
P_{1,n} & 0 & T_n^{3.1} & T_n^{3.2} & T_n^{3.3} & T_n^{3.4} & 0 & 0 & T_n^{3.7} & T_n^{3.8} & T_n^{3.9} & T_n^{3.10} \\
0 & P_{2,n} & 0 & 0 & 1 & 0 & 0 & 0 & 0 & 0 & 0 & 0 \\
P_{3,n} & 0 & T_n^{4.1} & T_n^{4.2} & T_n^{4.3} & T_n^{4.4} & 0 & 0 & T_n^{4.7} & T_n^{4.8} & T_n^{4.9} & T_n^{4.10} \\
0 & P_{4,n} & 0 & 0 & 0 & 1 & 0 & 0 & 0 & 0 & 0 & 0 \\
0 & 0 & T_n^{5.1} & T_n^{5.2} & T_n^{5.3} & T_n^{5.4} & 0 & 0 & T_n^{5.7} & T_n^{5.8} & T_n^{5.9} & T_n^{5.10} \\
0 & 0 & T_n^{6.1} & T_n^{6.2} & T_n^{6.3} & T_n^{6.4} & 0 & 0 & T_n^{6.7} & T_n^{6.8} & T_n^{6.9} & T_n^{6.10} \\
0 & 0 & T_n^{9.1} & T_n^{9.2} & T_n^{9.3} & T_n^{9.4} & P_{1,n} & 0 & T_n^{9.7} & T_n^{9.8} & T_n^{9.9} & T_n^{9.10} \\
0 & 0 & 0 & 0 & 0 & 0 & 0 & P_{2,n} & 0 & 0 & 1 & 0 \\
0 & 0 & T_n^{10.1} & T_n^{10.2} & T_n^{10.3} & T_n^{10.4} & P_{3,n} & 0 & T_n^{10.7} & T_n^{10.8} & T_n^{10.9} & T_n^{10.10} \\
0 & 0 & 0 & 0 & 0 & 0 & 0 & P_{4,n} & 0 & 0 & 0 & 1 \\
0 & 0 & T_n^{11.1} & T_n^{11.2} & T_n^{11.3} & T_n^{11.4} & 0 & 0 & T_n^{11.7} & T_n^{11.8} & T_n^{11.9} & T_n^{11.10} \\
0 & 0 & T_n^{12.1} & T_n^{12.2} & T_n^{12.3} & T_n^{12.4} & 0 & 0 & T_n^{12.7} & T_n^{12.8} & T_n^{12.9} & T_n^{12.12}
\end{bmatrix},$$

$$\mathbf{W}_n = \left[P_{5,n}, 0, P_{6,n}, 0, 0, 0, 0, 0, 0, 0, 0, 0\right]^T,$$

where

$$P_{1,n} = -k_r \varepsilon_n i^{n-1} H_n^{(1)'}(k_r a_q)/\omega a_q,$$
$$P_{2,n} = -K_r \varepsilon_n i^{n-1} J_n'(K_r a_0)/\omega a_q,$$
$$P_{3,n} = -\omega \rho_1 \varepsilon_n i^{n+1} H_n^{(1)}(k_r a_q)/c_{44},$$
$$P_{4,n} = \omega \rho_2 \varepsilon_n i^{n+1} J_n(K_r a_0)/c_{44},$$
$$P_{5,n} = \varphi_0 k_r \varepsilon_n i^{n-1} J_n'(k_r a_q)/\omega a_q,$$
$$P_{6,n} = \omega \rho_1 \varphi_0 \varepsilon_n i^{n+1} J_n(k_r a_q)/c_{44},$$

and $T_n^{i,j}z$ $(i, j = 1, 2, ..., 12)$ are elements of the modal transfer matrix, n.

APPENDIX III

$$\mathbf{G}_n^{\pm} = \begin{bmatrix}
\mathbf{G}_{n,11}^{\pm} & \mathbf{G}_{n,12}^{\pm} & \mathbf{G}_{n,13}^{\pm} \\
\mathbf{G}_{n,21}^{\pm} & \mathbf{G}_{n,22}^{\pm} & \mathbf{G}_{n,23}^{\pm} \\
\mathbf{G}_{n,31}^{\pm} & \mathbf{G}_{n,32}^{\pm} & \mathbf{G}_{n,33}^{\pm}
\end{bmatrix},$$

where

$$\mathbf{G}_{n,11}^{\pm} = \begin{bmatrix} 0 & 0 \\ 0 & \frac{1}{\eta} \end{bmatrix}, \mathbf{G}_{n,12}^{\pm} = \begin{bmatrix} -ia_q k_z & 0 \\ \mp\frac{in}{\eta} & 0 \end{bmatrix}, \mathbf{G}_{n,13}^{\pm} = \begin{bmatrix} -\frac{c_{56}}{\kappa_1} & \frac{c_{66}}{\kappa_1} \\ \frac{c_{55}}{\kappa_1} & -\frac{c_{56}}{\kappa_1} \end{bmatrix}, \mathbf{G}_{n,23}^{\pm} = \begin{bmatrix} 0 & 0 \\ \mp\frac{in}{\eta} & -ik_z a_q \end{bmatrix},$$

$$\mathbf{G}_{n,21}^{\pm} = \begin{bmatrix} -\frac{c_{13} ik_z a_q}{c_{11}} \mp \frac{c_{14} in}{c_{11}\eta} & -\frac{c_{14} ik_z a_q}{c_{11}} \mp \frac{c_{12} in}{c_{11}\eta} \\ \pm\frac{\kappa_2 in}{\eta^2} + \frac{\kappa_3 ik_z a_q}{\eta} & \pm\frac{\kappa_4 in}{\eta^2} + \frac{\kappa_2 ik_z a_q}{\eta} \end{bmatrix}, \mathbf{G}_{n,22}^{\pm} = \begin{bmatrix} -\frac{c_{12}}{c_{11}\eta} & \frac{c_{44}}{c_{11}} \\ \frac{\kappa_4}{\eta^2} - \frac{\rho_c a_q^2 \omega^2}{c_{44}} & \frac{1}{\eta}\left(\frac{c_{12}}{c_{11}} - 1\right) \end{bmatrix},$$

$$\mathbf{G}_{n,31}^{\pm} = \begin{bmatrix} \kappa_5 k_z^2 a_q^2 \pm \frac{k_z a_q n}{c_{44}\eta}(\kappa_3 + \kappa_6) + \frac{\kappa_2 n^2}{\eta^2} & \frac{-\rho_c a_q^2 \omega^2}{c_{44}} \pm \frac{2k_z a_q n \kappa_2}{\eta} + \kappa_6 k_z^2 a_q^2 + \frac{\kappa_4 n^2}{\eta^2} \\ \frac{-\rho_c a_q^2 \omega^2}{c_{44}} + \frac{\kappa_6 n^2}{\eta^2} + \kappa_7 k_z^2 a_q^2 \pm \frac{2\kappa_5 k_z a_q n}{\eta} & \frac{\kappa_2 n^2}{\eta^2} \pm \frac{k_z a_q n}{\eta}(\kappa_3 + \kappa_6) + \kappa_5 k_z^2 a_q^2 \end{bmatrix},$$

$$\mathbf{G}^{\pm}_{n,32} = \begin{bmatrix} -\frac{\kappa_2 i k_z a_q}{\eta} & \mp\frac{\kappa_4 i n}{\eta^2} & \mp\frac{c_{12} i n}{c_{11}\eta} & -\frac{c_{14} i k_z a_q}{c_{11}} \\ \mp\frac{\kappa_2 i n}{\eta^2} & -\frac{\kappa_3 i k_z a_q}{\eta} & \mp\frac{c_{14} i n}{c_{11}\eta} & -\frac{c_{13} i k_z a_q}{c_{11}} \end{bmatrix}, \quad \mathbf{G}^{\pm}_{n,33} = \begin{bmatrix} -\frac{2}{\eta} & 0 \\ 0 & -\frac{1}{\eta} \end{bmatrix}.$$

REFERENCES

1. M. Talmant and H. Batard, Proc. IEEE Ultrasonic Sym. **3**, 1371 (1994).
2. A. Migliori and J. L. Sarrao, *Resonant Ultrasound Spectroscopy: Applications to Physics, Materials Measurements and Nondestructive Evaluation* (Wiley, New York, 1997).
3. J. Y. Kim and J. G. Ih, Appl. Acoust. **64**, 1187 (2003).
4. S. M. Hasheminejad and M. Rajabi, Ultrasonics, **47**, 32 (2007).
5. F. Honarvar and A. N. Sinclair, Ultrasonics **36**, 845 (1998).
6. M. Rajabi and S. M. Hasheminejad, Ultrasonics, **49**, 682 (2009).
7. A. A. Kleshchev, Acoust. Phys. **60**, 279 (2014).
8. A. Tesei, W. L. J. Fox, A. Maguer, and A. Lovik, J. Acoust. Soc. Am. **108**, 2891 (2000).
9. D. Guicking, K. Goerk, and H. Peine, Proc. of SPIE – Int. Soc. Optic. Eng. **1700**, 2 (1992).
10. L. Flax, L. R. Dragonette, and H. Uberall, J. Acoust. Soc. Am. **63**, 723 (1978).
11. J. D. Murphy, E. D. Breitenbach, and H. Uberall, J. Acoust. Soc. Am. **64**, 678 (1978).
12. G. C. Gaunaurd, App. Mech. Rev. **42**, 143 (1989).
13. H. Uberall, *Acoustic Resonance Scattering* (Gordon and Breach Sci., Philadelphia, 1992).
14. N. D. Veksler, *Resonance Acoustic Spectroscopy. Springer Series on Wave Phenomena* (Springer-Verlag, Berlin, 1993).
15. J. J. Faran, J. Acoust. Soc. Am. **23**, 405 1951).
16. L. Flax, G. C. Gaunaurd, and H. Uberall, in *Physical Acoustics*, Ed. by W. P. Mason and R. N. Thurston (New York, 1981), Vol. 15, Chap. 3, pp. 191–294.
17. F. Honarvar and A. N. Sinclair, J. Acoust. Soc. Am. **100**, 57 (1996).
18. G. Kaduchak and C. M. Loeffler, J. Acoust. Soc. Am. **99**, 2545 (1996).
19. F. Ahmad and A. Rahman, Int. J. Eng. Sci. **38**, 325 (2000).
20. A. A. Kleshchev, Open J. Acoust. **3**, 67 (2013).
21. A. A. Kleshchev, Adv. Signal Proc. **1**, 44 (2013).
22. N. B. Karabutov, Podymova, and I. O. Belyaev, Acoust. Phys. **59**, 667 (2013).
23. N. V. Polikarpova, P. V. Mal'neva, and V. B. Voloshinov, Acoust. Phys. **59**, 291 (2013).
24. A. D. Pierce, *Acoustics: An Introduction to Its Physical Principles and Applications* (Am. Inst. Phys., New York, 1991).
25. J. D. Achenbach, *Wave Propagation in Elastic Solids* (North-Holland, New York, 1976).
26. S. G. Lekhnitsky, *The Theory of Elasticity of an Anisotropic Body* (Mir, Moscow, 1981), [in Russian], 2nd ed.
27. E. L. Shenderov, *Emission and Scattering of Sound* (Sudostroenie, Leningrad, 1989) [in?Russian].
28. M. S. Choi, Y. S. Joo, and J. Lee, J. Acoust. Soc. Am. **99**, 2594 (1996).
29. M. S. Choi, J. Korean Phys. Soc. **37**, 519 (2000).
30. M. Rajabi and M. Behzad, Composite Struct. **116**, 747 (2014).
31. M. Rajabi, M. T. Ahmadian, and J. Jamali, Composite Struct. **128**, 395 (2015).